MDPI

*Article*

# Evaluation of Antioxidant, Cytotoxic, Mutagenic and Other Inhibitory Potentials of Green Synthesized Chitosan Nanoparticles

Narayanasamy Duraisamy [1], Sangeetha Dhayalan [1,*], Mohammed Rafi Shaik [2,*], Althaf Hussain Shaik [3], Jilani P. Shaik [4] and Baji Shaik [5]

1 Department of Microbiology, Faculty of Science, Annamalai University, Annamalai Nagar, Chidambaram 608002, Tamil Nadu, India
2 Department of Chemistry, College of Science, King Saud University, Riyadh 11451, Saudi Arabia
3 Department of Zoology, College of Science, King Saud University, P.O. Box 2454, Riyadh 11451, Saudi Arabia
4 Department of Biochemistry, College of Science, King Saud University, Riyadh 11451, Saudi Arabia
5 School of Chemical Engineering, Yeungnam University, Gyeongsan 38541, Korea
* Correspondence: ds13134@annamalaiuniversity.ac.in (S.D.); mrshaik@ksu.edu.sa (M.R.S.);
  Tel.: +91-9486680815 (S.D.); +966-11-46-70439 (M.R.S.)

**Abstract:** The current study was performed with aim of evaluating antioxidant, cytotoxicity, $\alpha$-amylase, and $\alpha$-glucosidase inhibitory activities and mutagenicity properties of *Martynia annua* mediated Chitosan nanoparticles (MAL-CNPs). The green synthesized MAL-CNPs were characterized and confirmed through several characterization techniques, including UV-visible spectroscopy (UV-Vis), high-resolution transmission electron microscopy (HRTEM), scanning electron microscopy (SEM), Fourier-transform infrared spectroscopy (FT-IR), and dynamic light scattering (DLS). The HR-TEM analysis exhibited that the as-synthesized chitosan nanoparticles are spherical in shape. Furthermore, the DLS analysis exhibited that the average size of MAL-CNPs was 53 nm and the maximum diameter was 130.7 nm. The antioxidant activity results revealed that the MAL-CNPs showed DPPH (2,2-diphenyl-1-picrylhydrazyl) (66.78%) and $H_2O_2$ (91.65%) scavenging activities at 50 $\mu$g/mL concentration. The $IC_{50}$ values were 2.431 $\mu$g/mL and 50 $\mu$g/mL for DPPH and $H_2O_2$, respectively. MTT (3-4, 5 dimethylthiazol-2yl-2, 5-diphenyltetrazolium bromide) assay results exhibited dose-dependent cytotoxicity found from 50 $\mu$g/mL concentration of MAL-CNPs. The MAL-CNPs showed remarkable $\alpha$-glucosidase and $\alpha$-amylase inhibitory activity ($IC_{50}$ 1.981 $\mu$g/mL and 161.8 $\mu$g/mL). No toxic effect of MAL-CNPs was found through the Ames test. Further, the study concluded that MAL-CNPs are non-toxic and possess adequate antioxidants and cytotoxicity activity against cancer cells, $\alpha$-glucosidase, and $\alpha$-amylase inhibitory activity. Hence, the MAL-CNPs were considered for biomedical applications after the assessment of their efficiency and safety.

**Keywords:** *Martynia annua*; antioxidant activity; MTT assay; $\alpha$-glucosidase inhibitory assay

## 1. Introduction

Nanobiotechnology is an advanced research field that entails configuring, synthesizing, and applying particle sizes ranging from 1 to 100 nm [1]. In recent decades, the discovery of nanoparticles' distinctive attributes has enabled their use in various fields, including biomedicine, drug and gene delivery, antimicrobials, antioxidants, tumor detection, etc. [2]. Among different nanoparticles, chitosan is the most popular biodegradable nanoparticle as of yet. Chitosan nanoparticles have many therapeutic applications, including drug delivery, antidiabetic agents, wound healing, antimicrobial agents with the shipping carrier, and effective drug delivery control [3–5].

The potential of such polymer-based nanomaterials to combat particles with specialized surface receptors and enter cells can help with more efficient and secure regenerative

medicine [6]. As small generalized polypeptide adsorption properties, polymer nanoparticles, particularly some with a hydrophilic exterior, are widely used as carriers. Providentially, this chitosan polymeric compound occurs naturally in abundance [7–9]. Generally, chitosan has several applications due to its excellent phytochemical characteristics and distinctive applications, including healthcare, nourishment, chemical, cosmetic products, water purification, metal production and recovery, and metabolic and bioengineering industries [10].

Chitosan comprises a few functional groups that allow graft alteration, which confers special characteristics on the customized chitosan [11,12]. These improvements can be used to attain chemically altered chitosan to increase its solubility and thus broaden its biological applications. Such chemical modifications result in a wide range of chitosan derivatives with long-term release characteristics, nontoxicity, excellent biocompatibility, and compostability [11,13]. As a positively charged polymer, it has bio-adhesion, anti-hypercholesterolemic, cell membrane transfection, and anti-inflammatory properties that can be improved by blending this with other substances, making it an attractive candidate for biological and medical applications [14]. Moreover, chitosan nanoparticles can boost the immune system, resulting in antitumor activity. Additionally, chitosan nanoparticles are being used as drug delivery carriers due to their high biodegradability and biocompatibility and their convenience of modification [15,16]. The presence of hydroxyl and amino groups in chitosan makes it the ideal forum for complex formation with some other compounds, actively helping in the formation of more sustainable complexes with improved pharmacokinetics and pharmacodynamics [17]. Furthermore, the functional groups are abundant, and chitosan could be altered in various ways to produce swapped, covalently bonded, carboxylate, ionic, and enclosed derivative products to meet a variety of future research [18].

In this context, the medicinal plant, *Martynia annua* was used to synthesize chitosan nanoparticles (MAL-CNPs), hence it possessed pharmaceutical-grade precious phytochemical constituents and has been used to treat venomous bites, tuberculosis, and sore throats for decades [19]. Thus, the current research was framed to the synthesis of chitosan nanoparticles (MAL-CNPs) with *Martynia annua* extract to evaluate their in vitro antioxidant, cytotoxic, α-amylase, α-glucosidase, and mutagenicity properties (Scheme 1).
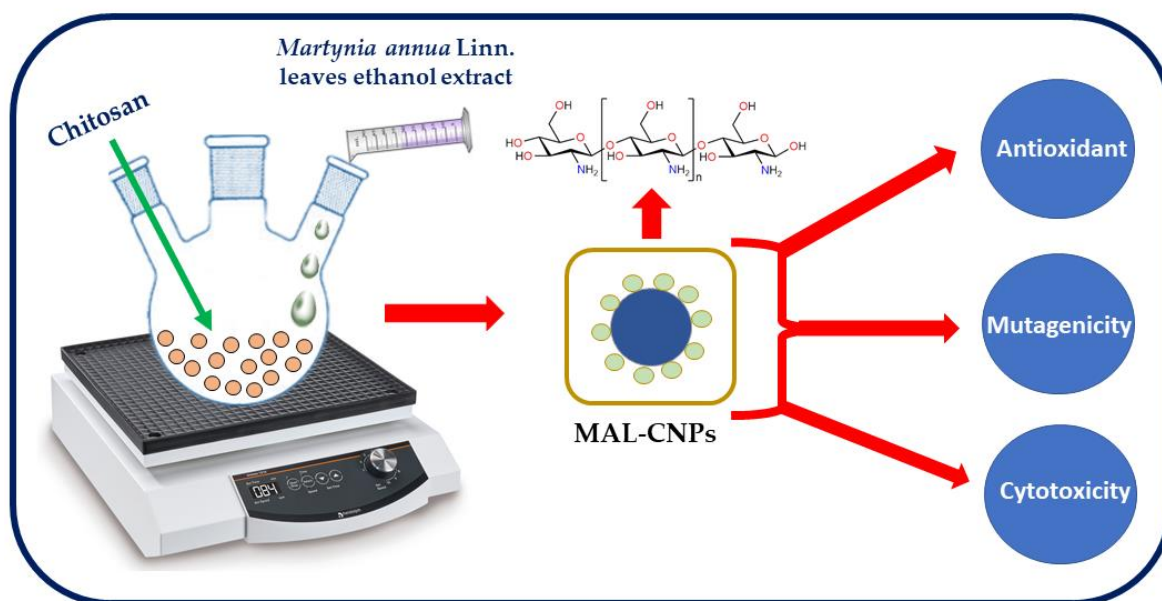


**Scheme 1.** Schematic representation of green synthesized chitosan nanoparticles (MAL-CNPs) using *Martynia annua* extract and its biomedical applications.

## 2. Materials and Methods

### 2.1. Materials

The healthy leaves of the *Martynia annua* sample were collected from East Rajapalayam, Salem District, Tamil Nadu, India. The collected plant was identified and recognized as *Martynia annua* by Professor P. Jayaraman, Director, Plant Anatomy Research Centre Chennai, Tamil Nadu (Reg. No. of Certificate: PARC/2020/4375). The collected leaf sample was rinsed with clean tap water to remove dirt and shadow-dried until it was completely dehydrated. The well-dried leaf sample was pulverized using an electric mixer and sieved through a standard flour filter. Chitosan, ethanol, acetic acid, and other solvents used in this work were purchased from Sigma Aldrich, St. Louis, MO, USA.

### 2.2. Leaf Extract Preparation

The standard hot plate extraction approach was maintained to attain extreme yield with vital phytochemicals [20]. Approximately 5 g of fine powdered *Martynia annua* leaf sample was added separately to 25 mL of ethanol, hexane, chloroform, methanol, and water. The sample comprising solvent blends was heated at 70 °C for 1 h. After the extraction procedure, the solvent extract was filtered and then concentrated using a vacuum evaporator (Heidolph vacuum evaporator, Model:G3; Schwabach, Germany). Each solvent extract yield was assessed using the following principle:

$$\text{Extract yield}(\%) = \frac{(\text{Weight of beaker with extract(g)}) - (\text{Weight of beaker without extract (g)})}{\text{Sample weight (g)}}$$

### 2.3. Synthesis of Chitosan Nanoparticles

Approximately 10 mL of 1% organic chitosan (dissolved in acetic acid: $v/v$) was mixed with 10 mL of ethanol extract and incubated for 1 h at 50 °C in an orbital shaker at 100 rpm. The turbidity of the reaction mixture was centrifuged after incubation at 10,000 rpm for 10 min. The supernatant was discarded, and subsequent centrifugation and rinsing of the pellets with an acetic acid solution (to remove un-synthesized nanoparticles) was performed. After subsequent centrifugation, the chitosan nanoparticles (MAL-CNPs) were freeze-dried and subjected to further characterization techniques [21].

### 2.4. Characterization of MAL-CNPs

The freeze-dried MAL-CNPs were suspended in acetic acid (1%), and their spectral absorbance was recorded on a UV-visible spectrophotometer (ASK Lab Instruments, Hyderabad, India). The functional groups (responsible for reduction, capping, and stabilization) present over the surface of MAL-CNPs were analyzed by following typical FT-IR protocol, and the frequency band was scanned in the range 400–4000 cm$^{-1}$ using Nicolet (iS50) FT-IR (Thermo Fisher, St. Louis, MO, USA). Dynamic light scattering (DLS) was performed on the Malvern panalytical instrument, Malvern, Worcestershire, United Kingdom. The HRTEM analysis of MAL-CNPs was carried out using JEOL Model JEM2100F at an operating voltage of 200 kV, Tokyo, Japan. SEM analysis was performed using SEM (ZEISS), Jena, Germany.

### 2.5. Phytochemical Qualitative Study

The ethanol extract of *Martynia annua* was examined for phytochemical investigation using extract yield and thin layer chromatography (TLC) analyses. The typical phytochemical properties, such as alkaloids (Dragendorff's), terpenoids (Salkowski test), carbohydrates (Benedict's), glycosides (Keller-Kilani test), flavonoids (Zinc-HCl reduction test), protein and amino acids (Millon's test), tannin and phenol (FeCl$_2$ test), saponin (Froth test), quinones (Borntrager's test), fixed oil (paper test), resins (Acetone test), coumarins (Fluorescence test), and carotenoids were qualitatively examined with typical procedures [22,23].

### 2.6. Antioxidant Activity Competence Analysis

#### 2.6.1. DPPH Assay

The free radicals scavenging potential of *Martynia annua* extract-mediated CNPs (MAL-CNPs) was investigated by the following methodology of Narayanan et al. [20] with minor changes. Briefly, 100 μL of freshly prepared DPPH (0.1 mM) solution was mixed with 300 μL of different concentrations (500, 250, 100, 50, and 10 μg/mL) of chitosan nanoparticles (in triplicate) and shaken vigorously, then kept at room temperature for 30 min. After 30 min of incubation, the absorbance of each concentration reaction blend was recorded at 517 nm using a UV-vis spectrophotometer, and ascorbic acid was used as control. The following formula was applied to calculate the DPPH radicals scavenging percentage, and linear regression analysis was performed to calculate the $IC_{50}$ values.

$$\text{DPPH scavenging (\%)} = \frac{(\text{Absorbance of control} - \text{Absorbance of reaction mixture})}{\text{Absorbance of control}} \times 100$$

#### 2.6.2. $H_2O_2$ Scavenging Assay

The typical methodology was followed to evaluate the $H_2O_2$ scavenging potential of MAL-CNPs [24]. Concisely, 0.6 mL of 43 mM of $H_2O_2$ (1 M of phosphate buffer: pH 7.4) was mixed with 1.4 mL of various dosages, such as 500, 400, 300, 200, 100, 80, 60, 40, 20, and 10 μg/mL (individually) of MAL-CNPs. Subsequently, each reaction mixture was kept undisturbed for 15 min at room temperature, and the absorbance of each of them was measured with a UV-visible spectrophotometer at 230 nm. Furthermore, the $H_2O_2$ scavenging percentage and $IC_{50}$ were calculated through the standard formula and linear regression analyses.

$$\text{H}_2\text{O}_2 \text{ scavenging (\%)} = \frac{(\text{Absorbance of control} - \text{Absorbance of reaction mixture})}{\text{Absorbance of control}} \times 100$$

### 2.7. In Vitro Cytotoxic Assay

The cytotoxic property of MAL-CNPs was determined by following the standard MTT (3-(4,5-dimethylthiazol-2-yl)-2,5-diphenyl-2H-tetrazolium bromide) assay on RIN-m5F (Rat Islet Cells) cell line (procured from NCCS, Pune, India). Briefly, 200 μL of ($1 \times 10^5$ cells/mL/well) RIN-m5F cells were placed into a 96-well plate containing a DMEM medium. After incubation, the wells were rinsed with PBS and then treated with various concentrations (500, 400, 300, 200, 100, 80, 60, 40, 20, and 10 μg/mL) of MAL-CNPs in triplicate and then incubated at 37 °C in a 5% $CO_2$ (humidified) incubator for 24 h. After incubation, approximately 20 μL of MTT (5 mg/mL) was added to each well and again incubated for 4 h until the formations of purple color precipitated. Next, fluids from the wells were completely aspirated and washed with 200 μL of 1X PBS, then formazan crystals were dissolved with 100 μL of DMSO and shaken for 5 min. Subsequently, the absorbance of each well was recorded using a microplate reader (Thermo Fisher Scientific, Franklin, MA, USA) at 570 nm, and the percentage cell viability and $IC_{50}$ values were determined with standard formulas.

$$\text{Cell viability (\%)} = \frac{\text{Test OD}}{\text{Control OD}} \times 100 \tag{1}$$

### 2.8. α-Amylase Inhibitory Assay

The α-amylase inhibitory activity competence of MAL-CNPs was evaluated through the standard protocol of Shao et al. [25] with slight modifications. Briefly, approximately 100 μL of different dosages (500, 250, 100, 50, and 25 μg/mL) of MAL-CNPs were individually blended with 200 μL of freshly prepared α-amylase solution and kept undisturbed for 35 min at 25 °C. Subsequently, 400 μL of newly prepared 0.25% starch solution was mixed with each sample tube and left undisturbed for 5 min at 37 °C. Next, 1.0 mL of the DNS solution was blended to inhibit the reaction and then left in a water bath (10 min)

and chilled to room conditions. The acarbose was used as a positive control, and the absorbance of each sample reaction was read at 540 nm. The following formula and linear regression analysis were applied to calculate the $\alpha$-amylase inhibitory percentage and $IC_{50}$ values, respectively.

$$\alpha\text{-Amylase Inhibition (\%)} = \frac{\text{A control} - (\text{A test} - \text{A background})}{\text{Control}} \times 100$$

### 2.9. α-Glucosidase Inhibitory Assay

The standard protocol [25] with slight modifications was followed to assess the $\alpha$-glucosidase inhibitory efficiency of MAL-CNPs. Briefly, approximately 60 µL of various dosages (500, 250, 100, 50, and 25 µg/mL) of MAL-CNPs were individually blended with 50 µL of $\alpha$-glucosidase solution (0.2 U/mL: prepared in 0.1 M of phosphate buffer: pH 6.8) in 96 well plates. These reaction mixtures were incubated at 37 °C for 30 min. After incubation, approximately 50 µL of 5 mM ρ-nitrophenyl-$\alpha$-D-glucopyranoside (PNPG) solution was added to each reaction mix and incubated at 37 °C for 20 min. Next, approximately 160 µL of 0.2 M $NaCO_3$ was added to each well to inhibit the reaction. Subsequently, the absorbance of each well was measured at 405 nm using a microplate reader and compared to positive control acarbose. The $\alpha$-glucosidase inhibitory efficiency was calculated following the formula, and the $IC_{50}$ value was determined by linear regression analysis.

$$\alpha\text{-Glucosidase Inhibition (\%)} = \frac{\text{Aco} - \text{At}}{\text{Aco}} \times 100$$

### 2.10. Mutagenicity Assay

The mutagenicity properties of MAL-CNPs were assessed by a typical Ames assay according to Organization for Economic co-operation and Development (OECD 471) [26]. Trial I (plate incorporation technique) and trial II (pre-incubation technique) were followed with various strains (TA 1535, TA 1537, TA 98, TA 100, and WP2) (trp pKM101) of *Salmonella typhimurium* and *E. coli* in the presence and absence of metabolic activator (+S9 and −S9) in triplicate. The different concentrations (0.125, 0.625, 1.25, 2.5, and 5 mg/plate) of MAL-CNPs were studied for both trial-I and trial-II as per OECD 471.

### 2.11. Statistical Analysis

All the data were analyzed with mean and standard deviation.

## 3. Results and Discussion

### 3.1. Plant Extract Yield and TLC Analysis

The several solvents (methanol, ethanol, hexane, chloroform, and water) hot plate-based extract preparation approach delivers diverse yield extents. Among these solvent extracts, ethanol provides an extreme yield in comparison with the other solvents. The ethanol solvent extract delivered an extreme yield of 0.43 g, and in percentage, it was measured as 8.68%; water extract yielded 0.39 g (7.98%), hexane 0.23 g (4.64%), methanol 0.27 g (5.42%), and chloroform 0.21 g (4.12%), as shown in Figure S1 (Supplementary File). The maximum yield of ethanol extracts proposes that they might comprise valuable photochemical compounds in comparison with other solvents. The TLC outcomes also showed that the ethanol extract displayed a superior number of visible spots than the other solvent extract under numerous visualization methods and had extreme Rf values with numerous colors visualized under various factors 255 nm and 365 nm, iodine, DPPH, 10% ferric chloride, visible light, Dragendorff's reagent, and concentrated sulfuric acid. The results report that the ethanol solvent efficiently extracts several bioactive phytochemicals from the *Martynia annua* Linn. leaf sample. According to a previous report, Kaushik et al. [27] attained approximately 19% of ethanol extract yield from the *Martynia annua* fruit sample. The plant extract increased yield for a specific solvent designates that the solvent

precise phytochemicals are enhanced in that plant sample, and, in addition, its strength is associated with the polarity interaction of solvent properties and phytochemicals [28].

### 3.2. Screening of Qualitative Phytochemicals

Based on the outcomes attained from different solvent yields and TLC investigation, *Martynia annua* leaf ethanol extract phytochemical contents were qualitatively examined. Remarkably, the ethanol extract comprises pharmaceutically valuable phytochemicals, including alkaloid, tannin, phenol, protein, amino acids, saponin, glycosides, quinones, fixed oil, resins, and carotenoids, as exhibited in Table 1.

**Table 1.** Qualitative phytochemical screening of *Martynia annua* ethanol extract.

| Serial No. | Phytochemicals | Test | Ethanol Extract |
|:---:|:---|:---|:---:|
| 1 | Carbohydrate | Benedict's Test | − |
| 2 | Protein and Amino Acids | Millions Test | + |
| 3 | Alkaloid | Dragendorff's Test | + |
| 4 | Tannin and Phenol | Ferric Chloride Test | + |
| 5 | Flavonoids | Zn-HCl Test | − |
| 6 | Terpenoids | Salkowski Test | − |
| 7 | Saponin | Froth Test | + |
| 8 | Glycosides | Keller-Kilani Test | + |
| 9 | Quinons | NaOH Test | + |
| 10 | Fixed Oil | Paper/spot Test | + |
| 11 | Resins | Acetone Test | + |
| 12 | Coumarins | Fluorescence Test | − |
| 13 | Carotenoids | NA | + |

Note: (+) means presence of phytochemical and (−) absence of phytochemical.

### 3.3. Chitosan Nanoparticle Synthesis and Characterization

#### 3.3.1. UV-Visible Analysis of MAL-CNPs

The ethanol leaf extract of *Martynia annua* displayed substantial chitosan nanoparticle (MAL-CNPs) fabricating potential. The Chitosan reducing the potential of this ethanol extract was primarily at peaks at 221, 232, and 319 nm (Figure 1). The peaks observed at these nanometer ranges were associated with the nanometer of MAL-CNPs. The UV-visible spectrum of MAL-CNPs are in the range 200–325 nm. These broad absorption bands are due to the existence of the CO group [29]. Oh et al. [30] reported that the UV-visible spectrum of MAL-CNPs using the ionic gelation approach noted the band at 320 nm and stated their antibacterial activity against phytopathogenic bacteria. The pure chitosan particle's UV-visible spectrum is 339 nm [31]. The UV-visible spectrum disparities of MAL-CNPs are directly associated with the process and synthesizing constraints followed for the MAL-CNPs synthesis approach [32].

#### 3.3.2. FT-IR Analysis

The functional groups involved in the reduction, capping, and stabilization of MAL-CNPs were inspected through FT-IR analysis (Figure 2). The numbers of major peaks at 3941, 3789, 3435, 2920, 2852, 2065, 1630, 1270, 1110, 1060, 1035, 875, 617, and 564 cm$^{-1}$ corresponded to various functional groups. The occurrence of peaks between 3940 and 3430 cm$^{-1}$ is associated with –NH$_2$ and –OH stretching vibrations, and it results in extra molecular bioactive molecules of H bonding. Correspondingly, the band noticed between 2920 and 2065 cm$^{-1}$ associated with the C-H stretching vibrations is related to aldehyde and alkane groups. The peaks noticed at 1635 cm$^{-1}$ correlated to the stretch of amide I, 1270 cm$^{-1}$ is attributed to –NH$_2$ bending, 1110–1035 cm$^{-1}$ is attributed to the amide III stretching vibrations, and 870–565 cm$^{-1}$ C-H bending connected to stretching of keto groups. A related FT-IR spectrum has been found for chitosan nanoparticles synthesized using *Achyranthes aspera* plant extract [33]. These outcomes indicate that the ethanol extract of *Martynia annua* comprises the most active compounds, which have the probability to

reduce the chitosan original form into chitosan nanoparticles. These phytochemicals play a significant role in the reduction, stabilization, and capping of chitosan nanoparticles [34].
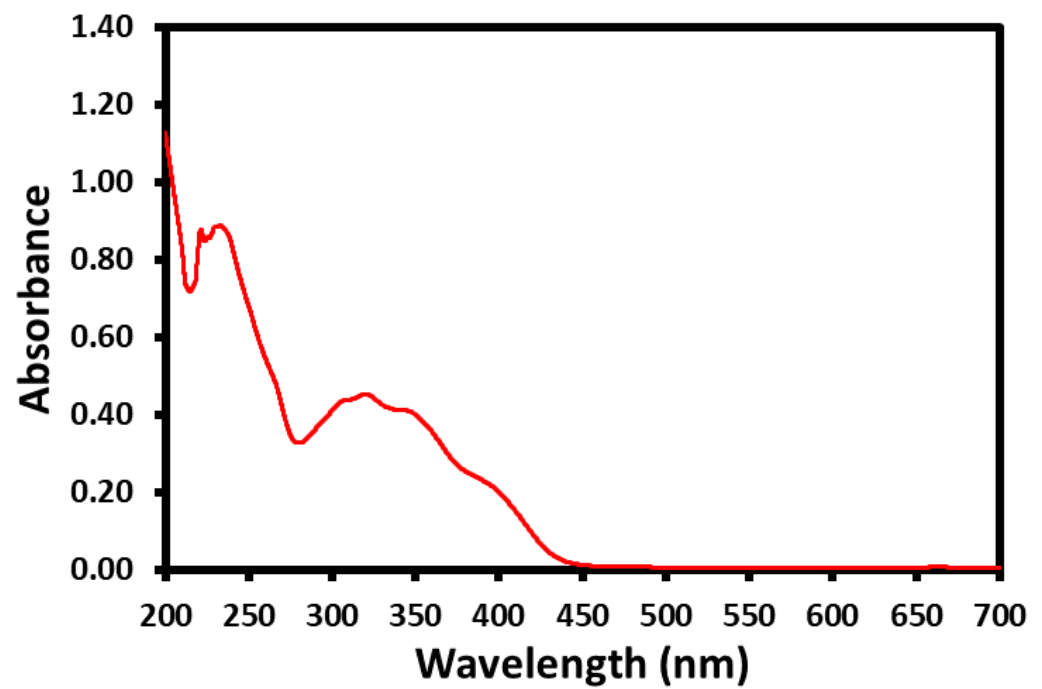


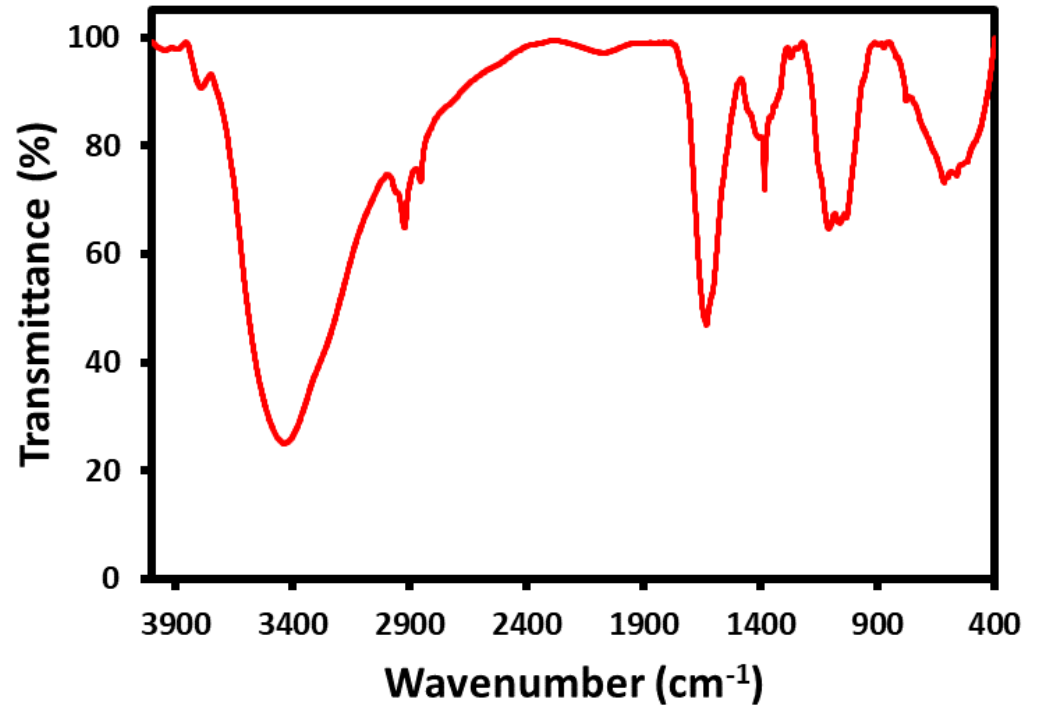**Figure 1.** UV-visible spectrum analysis of MAL-CNPs.



**Figure 2.** FT-IR analysis of MAL-CNPs.

### 3.3.3. HR-TEM Analysis

The size and morphology of as-synthesized chitosan nanoparticles (MAL-CNPs) with ethanolic leaf extract of *Martynia annua* plant are evaluated by using high-resolution transmission electron microscopic analysis (HR-TEM). The HR-TEM analysis showed the morphological properties and surface appearance of chitosan nanoparticles as being spherical in shape (Figure 3a, smooth surface, and size range of approximately 60–130 nm). The selected area electron diffraction (SAED) pattern illustrates characteristic rings (Figure 3b), which indicate that these chitosan nanoparticles are highly crystalline in nature. The average particle size of the chitosan nanoparticle is ~100–120 nm.
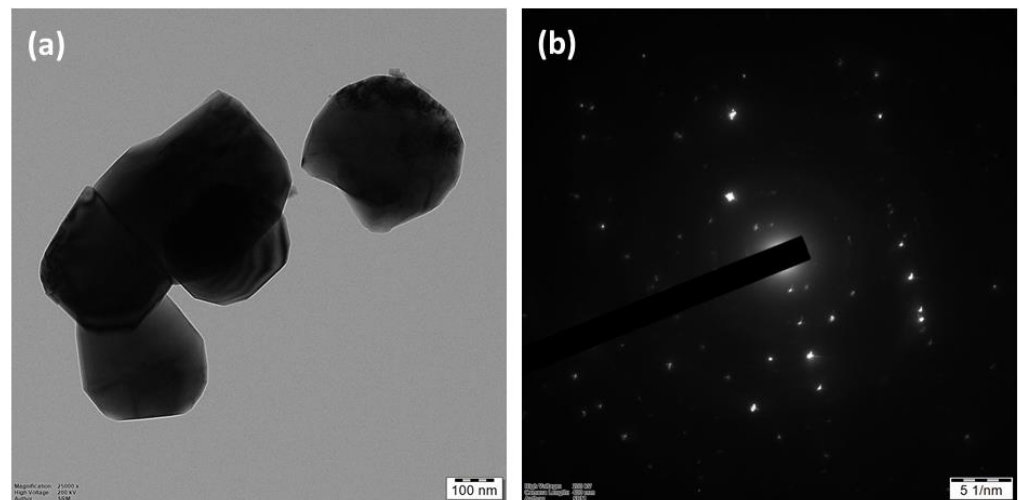


**Figure 3.** (**a**) HR-TEM image and (**b**) SAED pattern of MAL-CNPs.

### 3.3.4. SEM and DLS Analysis

The scanning electron microscopic (SEM) analysis of as-synthesized chitosan nanoparticles (MAL-CNPs) is further carried out to investigate the surface morphology of the MAL-CNPs (Figure 4a,b). It is revealed that relatively spherical and uniform MAL-CNPs are formed. The SEM images suggest the existence of organic moieties on the surface of nanoparticles as stabilizing agents. The accumulation of phytomolecules possibly occurs due to the hydrogen bonding and/or electrostatic interactions between the functional groups of active phytomolecules and the surface of chitosan nanoparticles. Furthermore, the DLS analysis exhibited that the average size of MAL-CNPs was 53 nm, maximum diameter was 130.7 nm, and the polydispersity index was found to be 0.315 (Figure 5, Supplementary File Table S1).
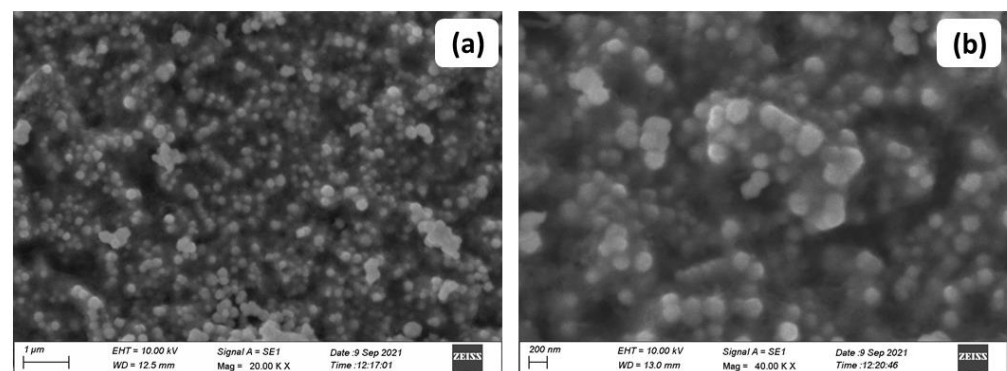


**Figure 4.** (**a**,**b**) Scanning electron microscopy of the MAL-CNPs at different magnifications.
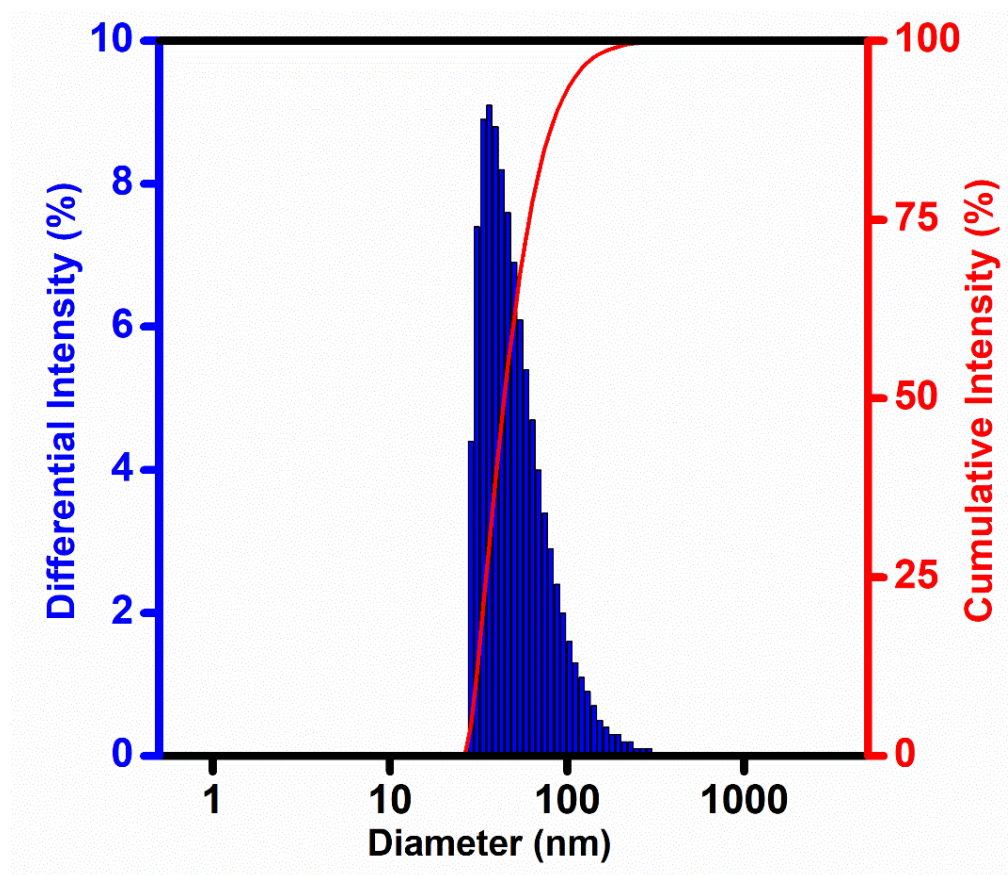
**Figure 5.** DLS analysis of MAL-CNPs.

*3.4. Antioxidant Activity Analysis*

The free radicals scavenging efficiency of MAL-CNPs was evaluated with DPPH and $H_2O_2$ scavenging assays. Figures 6 and 7 demonstrate the Optical Density and percentage of DPPH scavenging activities, respectively. A considerable DPPH radical scavenging rate of approximately 66.78% was found at a 50 μg/mL concentration of MAL-CNPs. The $IC_{50}$ value was found to be 2.431 μg/mL. This scavenging percentage was better than the DPPH scavenging efficiency of ascorbic acid (34.62%) (Figure 6). Similarly, Figure 7 represents $H_2O_2$ scavenging percentages of various concentrations of MAL-CNPs. Obtained results revealed that the 50 μg/mL concentration of MAL-CNPs showed approximately 91.65% of $H_2O_2$ scavenging potential. Interestingly, it was considerably more significant than the $H_2O_2$ scavenging percentage (90.91%) of the positive control (Figure 7). These results strongly suggest that the 50 μg/mL concentration of MAL-CNPs is the optimal value to donate the electron to convert the unstable radicals into stable radicals [35]. The bioactive compounds, which are involved in the synthesis, capping, and stabilization of MAL-CNPs and coated over their surface, might possess fine antioxidant activity by acting as electron donors. Such MAL-CNPs can improve free radical scavenging activity and also amplify the antioxidant activity of particles coated over their surface [36]. A similar pattern of antioxidant activity was reported by Kumar et al. [37] against DPPH and nitrate radicals. The antioxidants that donate electrons can convert the violet-colored DPPH into the yellow-colored diphenylpicryl hydrazine [38]. The MAL-CNPs can neutralize reactive oxygen species (ROS) in the micro-environments where it is incorporated, lowering cell-induced oxidative stress [39].
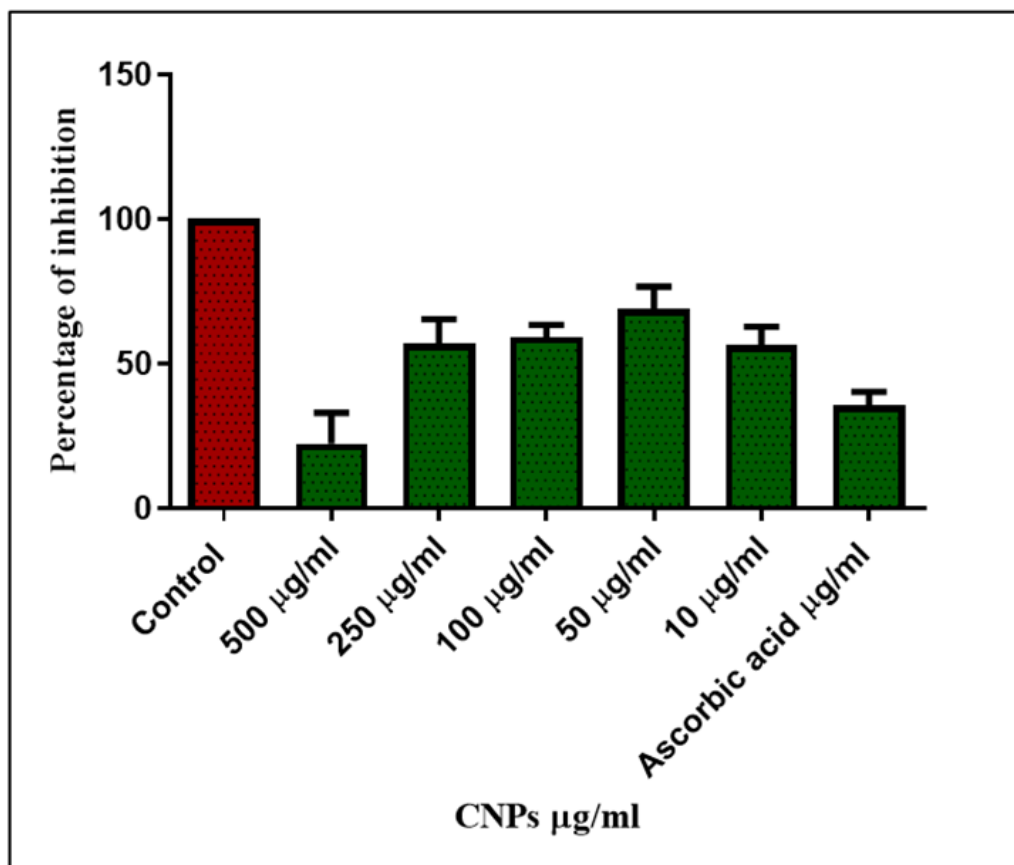
**Figure 6.** DPPH scavenging percentage of MAL-CNPs. Note: positive control: ascorbic acid; negative control: DPPH.
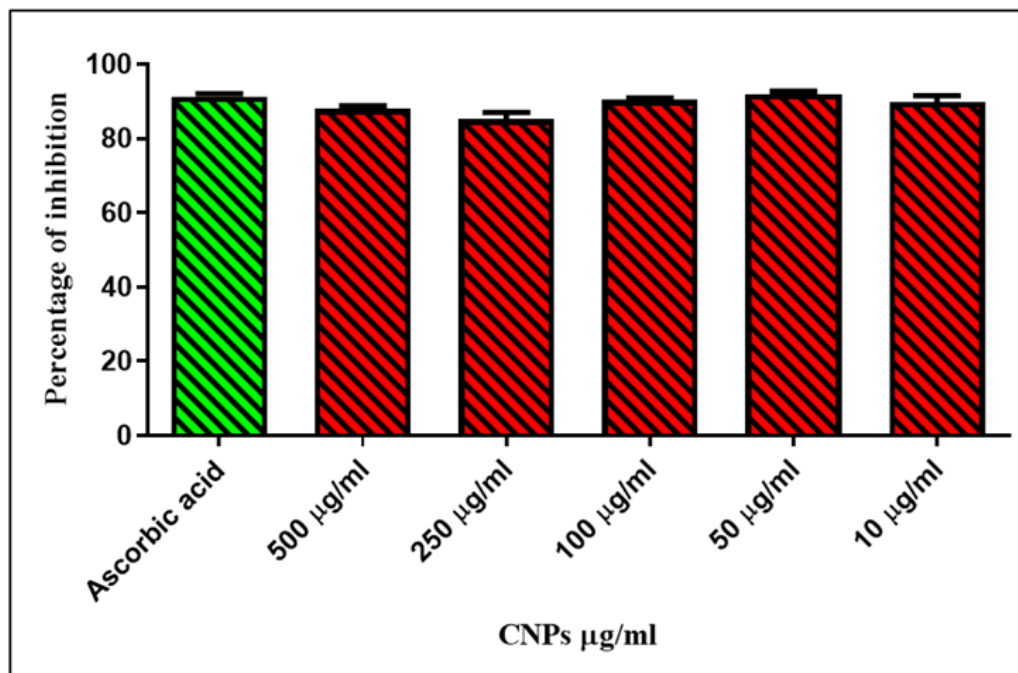


**Figure 7.** $H_2O_2$ scavenging percentage of MAL-CNPs.

### 3.5. Cytotoxic Property Analysis

The results obtained from the MTT assay are presented in Figures 8 and 9, which reveal the viability percentage and corresponding absorbance values of MAL-CNPs on RIN-m5F. The results suggest that the cell viability and cytotoxicity were dose-dependent. At minimum concentration (1–25 µg/mL), the cell viability was not affected by MAL-CNPs; therefore, cytotoxicity was recorded at increasing concentrations from 50 µg/mL. According to this, $IC_{50}$ was found to be 39.93 µg/mL. A report stated that chitosan-based nanoparticles showed a considerable level of cytotoxicity and yielded identical $IC_{50}$ and $IC_{20}$ values against the A549 cells. The cytotoxicity of chitosan nanoparticles was achieved by reducing the degree of polymer deacetylation, but it was less affected by decreasing the molecular weight [40]. Loutfy et al. [41] reported that chitosan-based nanoparticles showed cytotoxicity at increased concentration against the HepG2 cell, and they found that the $IC_{50}$ value was 239 µg/mL. Detailed analysis of the cytotoxic activity of the MAL-CNPs revealed a considerable impact on the apoptotic gene (caspase 3, p 53, and Bak) expression of mRNA [42]. The caspase 3 gene after the cell is exposed indicates the participation of an apoptotic caspase-independent route besides raising the exposure of the MAL-CNPs to a certain concentration [43].
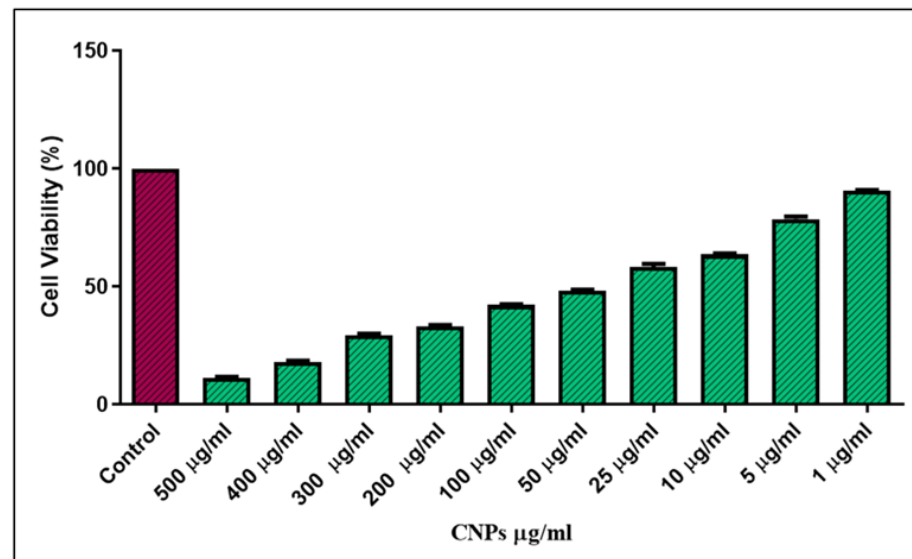


**Figure 8.** Cell viability percentage analysis by MTT assay with MAL-CNPs. Note: control: untreated cells.
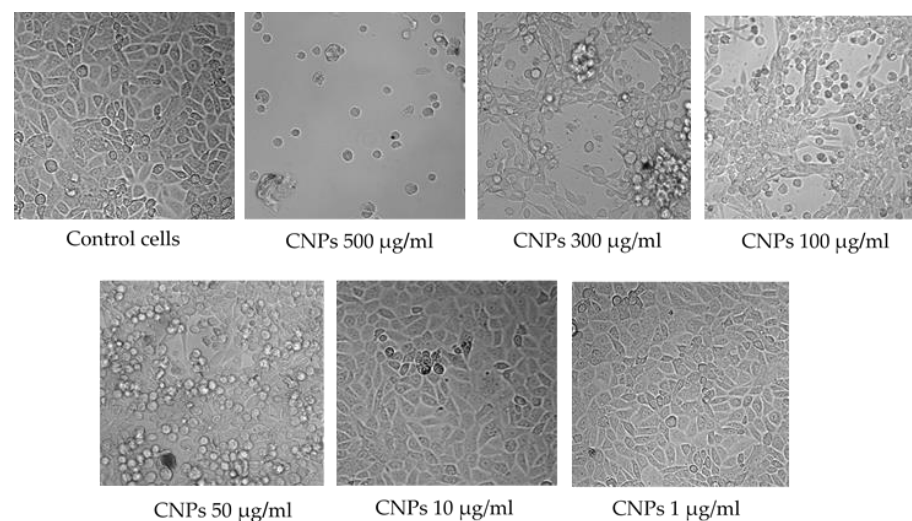


**Figure 9.** MTT assay with MAL-CNPs on treated cells.

### 3.6. α-Amylase Inhibitory and α-Glucosidase Inhibitory Assays

The substances α-amylase and α-glucosidase are the most essential inhibitory targets to control diabetic type II disease. Figure 10 depicts (OD and percentage of inhibition, respectively) the α-amylase inhibiting potential of MAL-CNPs. The obtained results suggest that the MAL-CNPs showed moderate inhibitory activity (3.38%) at 250 μg/mL concentration The IC$_{50}$ value was found to be 1.981 μg/mL. This inhibitory activity was reasonably comparable with the α-amylase inhibitory activity of acarbose (9.05 μg/mL). Similarly, the MA-CNPs also demonstrated considerable α-glucosidase inhibitory activity (Figure 11). The MAL-CNPs showed dose-dependent α-glucosidase inhibitory activity. An increased concentration (500 μg/mL) demonstrated maximum inhibition up to 33.88%. The IC$_{50}$ value was found to be 161.8 μg/mL. Interestingly, it was comparable with the inhibitory activity of the positive control (acarbose: 50.76%). This inhibition percentage gradually increased from 9.01 to 33.88% for 10–500 μg/mL concentration of MAL-CNPs. Similarly, *Pterocarpus marsupium* extract-mediated CNPs demonstrated a considerable percentage of dose-dependent α-amylase as well as α-glucosidase inhibitory activities [34]. Inhibiting such hydrolytic enzymes can help with type 2 diabetes treatment by lowering postprandial hyperglycemia [44].
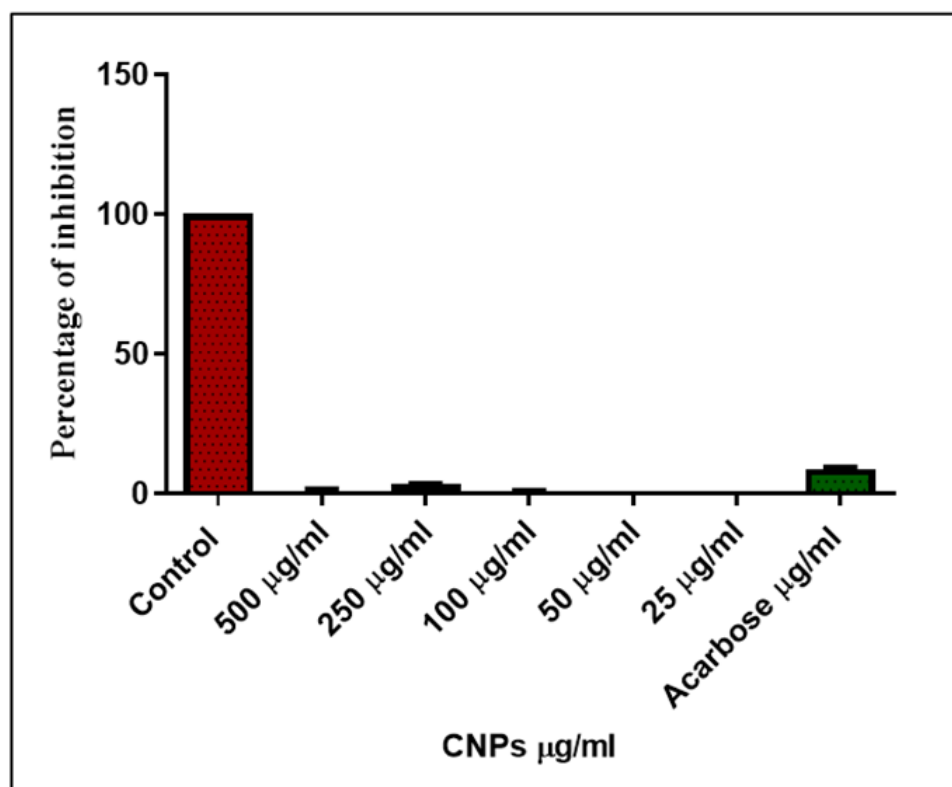


**Figure 10.** Percentage of α-amylase inhibitory activity assay with MAL-CNPs.

The bioactive compounds coated over the surface of MAL-CNPs are thought to be promising and efficient inhibitors of α-amylase as well as α-glucosidase. This study revealed that the MAL-CNPs inhibited α-amylase and α-glucosidase in a concentration-dependent [45] manner. The α-glucosidase had a more substantial inhibitory effect than α-amylase [46]. The apparent variation in the inhibition effect of α-amylase and α-glucosidase might lead to undigested sugars reaching the colon, resulting in intestinal microbial digestion and successive intestinal illnesses, including abdominal discomfort, constipation, and diarrhea [47].
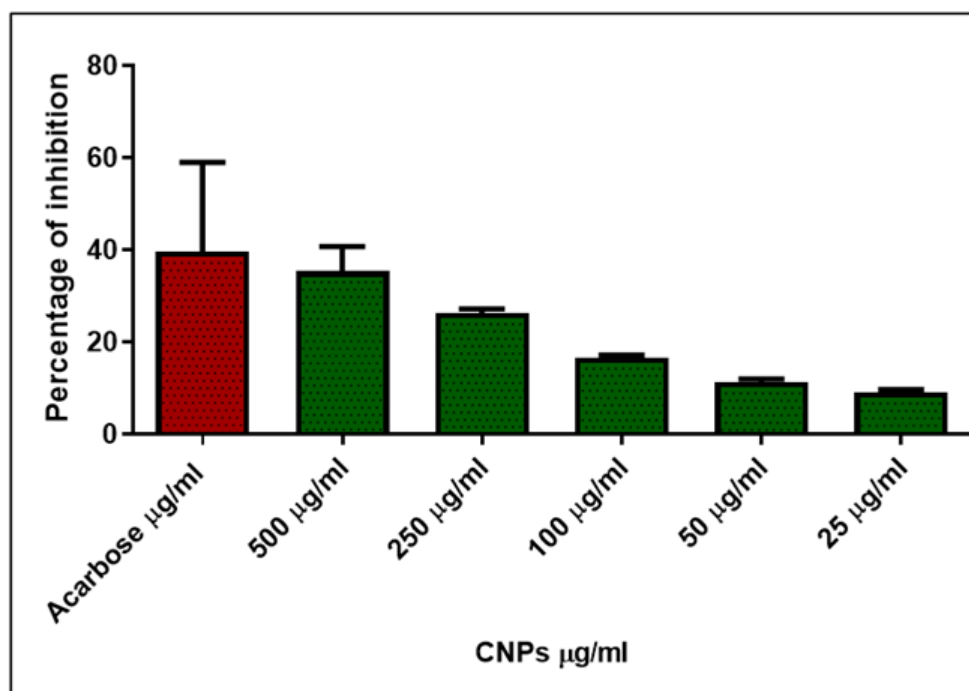
**Figure 11.** Percentage of α-glucosidase inhibitory activity assay with MAL-CNPs. Note: positive control: alphamylase + substrate; negative control: acarbose.

### 3.7. Mutagenicity Analysis

The mutagenicity property of MAL-CNPs against *Salmonella typhimurium* TA100 strain and *Escherichia coli* WP2 (trp pKM101) strain (out of five strains from each species) demonstrated slight toxicity. In the presence or absence of metabolic activation, there was no decrease in the revertant number of colonies inhibition compared to the negative control at any of the tested concentrations in either strain. According to the findings, 5 mg/plate was chosen as the highest proportion for such main study trials (trials I and II), both in the presence and absence of metabolic activation. The plate incorporation method was performed with five concentrations separated by a factor of two in triplicate of test items and the negative and positive controls with the three strains, i.e., TA 1537, TA1535, and TA98. For the remaining two tester strains, TA100 and WP2 (trp pKM101), cytotoxicity results were incorporated in Trial-I up to five concentrations.

Neither biologically substantial increase in revertant counts was noted from any of the five test strains pre-incubated with the test item in the absence or presence of metabolic activation. Either precipitation or reduction in background lawn was evidenced from any of the dosages investigated. The positive controls demonstrated an unambiguous rise in revertant counts, including all five test strains and corresponding controls, affirming the test system's sensitivity [48]. Based on these results, *Martynia annua*-mediated MAL-CNPs may indeed be non-mutagenic, as they did not stimulate gene mutation in any of the test strains at the concentrations tested. De Lima et al. [49] reported that the CNPs demonstrated no substantial changes in the mitosis process on human lymphocyte cells, and this suggests that the CNPs are non-toxic. The technique used demonstrates great potential to be used in nanoparticle safety checks, implying that these materials will be used in various biological and commercial applications in the future [50].

### 4. Conclusions

The present study aimed to evaluate the antioxidant, cytotoxicity, and mutagenic activity of green-synthesized MAL-CNPs. The obtained results conclude that the MAL-CNPs exhibited antioxidant activities, and this was confirmed by DPPH and $H_2O_2$ radicals scavenging assay. The MTT assay results revealed that the MAL-CNPs cytotoxicity activi-

ties were dose-dependent from the concentration of 50 μg/mL. The MAL-CNPs showed significant α-glucosidase and α-amylase inhibitory activity. These results indicate that these green synthesized MAL-CNPs may be considered as a valuable material for type 2 diabetic treatment. Furthermore, the Ames test results indicated that the MAL-CNPs were non-toxic, as they did not induce mutagenesis on bacterial test strains. These MAL-CNPs could be considered as therapeutic nanomaterials for several biomedical applications in the near future in medical fields. However, in-vivo studies need to be performed to ensure their efficiency and safety for future therapeutic applications.

**Supplementary Materials:** The following supporting information can be downloaded at: https://www.mdpi.com/article/10.3390/cryst12111540/s1, Figure S1: Different solvent extracts yield of *Martynia annua* Linn. stated values are mean and standard error of triplicates; Table S1: Volume Distribution Table of DLS Results.

**Author Contributions:** Conceptualization, N.D. and S.D.; methodology, N.D. and S.D.; formal analysis, M.R.S., A.H.S., J.P.S., and B.S.; investigation, N.D., S.D., and M.R.S.; resources, S.D.; data curation, N.D. and S.D.; writing—original draft preparation, N.D., S.D., and M.R.S.; writing—review and editing, N.D., S.D., and M.R.S.; supervision, S.D.; project administration, S.D.; funding acquisition, A.H.S. All authors have read and agreed to the published version of the manuscript.

**Institutional Review Board Statement:** Not applicable.

**Informed Consent Statement:** Not applicable.

**Data Availability Statement:** Data are contained within the article and supplementary file.

**Conflicts of Interest:** The authors declare no conflict of interest.

# References

1. Ratan, Z.A.; Haidere, M.F.; Nurunnabi, M.; Shahriar, S.M.; Ahammad, A.; Shim, Y.Y.; Reaney, M.J.; Cho, J.Y. Green chemistry synthesis of silver nanoparticles and their potential anticancer effects. *Cancers* **2020**, *12*, 855. [CrossRef] [PubMed]
2. Vallabani, N.; Singh, S. Recent advances and future prospects of iron oxide nanoparticles in biomedicine and diagnostics. *3 Biotech* **2018**, *8*, 279. [CrossRef] [PubMed]
3. Sur, S.; Rathore, A.; Dave, V.; Reddy, K.R.; Chouhan, R.S.; Sadhu, V. Recent developments in functionalized polymer nanoparticles for efficient drug delivery system. *Nano-Struct. Nano-Objects* **2019**, *20*, 100397. [CrossRef]
4. Othman, S.I.; Alturki, A.M.; Abu-Taweel, G.M.; Altoom, N.G.; Allam, A.A.; Abdelmonem, R. Chitosan for biomedical applications, promising antidiabetic drug delivery system, and new diabetes mellitus treatment based on stem cell. *Int. J. Biol. Macromol.* **2021**, *190*, 417–432. [CrossRef] [PubMed]
5. Subramaniam, S.; Kumarasamy, S.; Narayanan, M.; Ranganathan, M.; Rathinavel, T.; Chinnathambi, A.; Alahmadi, T.A.; Karuppusamy, I.; Pugazhendhi, A.; Whangchai, K. Spectral and structure characterization of Ferula assafoetida fabricated silver nanoparticles and evaluation of its cytotoxic, and photocatalytic competence. *Environ. Res.* **2022**, *204*, 111987. [CrossRef]
6. Chen, S.; Li, R.; Li, X.; Xie, J. Electrospinning: An enabling nanotechnology platform for drug delivery and regenerative medicine. *Adv. Drug Deliv. Rev.* **2018**, *132*, 188–213. [CrossRef]
7. Naqvi, S.; Panghal, A.; Flora, S. Nanotechnology: A promising approach for delivery of neuroprotective drugs. *Front. Neurosci.* **2020**, *14*, 494. [CrossRef]
8. Narayanan, M.; Deepika, M.; Ma, Y.; Nasif, O.; Alharbi, S.A.; Srinivasan, R.; Natarajan, D. Phyto-fabrication, characterization, and biomedical activity of silver nanoparticles mediated from an epiphytic plant Luisia tenuifolia Blume. *Appl. Nanosci.* **2021**, 1–11. [CrossRef]
9. Pugazhendhi, A.; Vasantharaj, S.; Sathiyavimal, S.; Raja, R.K.; Karuppusamy, I.; Narayanan, M.; Kandasamy, S.; Brindhadevi, K. Organic and inorganic nanomaterial coatings for the prevention of microbial growth and infections on biotic and abiotic surfaces. *Surf. Coat. Technol.* **2021**, *425*, 127739. [CrossRef]

10.  Anjum, S.; Komal, A.; Abbasi, B.H.; Hano, C. Nanoparticles as Elicitors of Biologically Active Ingredients in Plants. In *Nanotechnology in Plant Growth Promotion and Protection: Recent Advances and Impacts*; Wiley Online Library: New York, NY, USA, 2021; pp. 170–202.

11.  Wei, S.; Ching, Y.C.; Chuah, C.H. Synthesis of chitosan aerogels as promising carriers for drug delivery: A review. *Carbohydr. Polym.* **2020**, *231*, 115744. [CrossRef]

12.  Narayanan, M.; Natarajan, D.; Priyadharshini, S.G.; Kandasamy, S.; Shanmugam, S.; Sabour, A.; Almoallim, H.S.; Pugazhendhi, A. Biofabrication and characterization of AgNPs synthesized by Justicia adhatoda and efficiency on multi-drug resistant microbes and anticancer activity. *Inorg. Chem. Commun.* **2021**, *134*, 109071. [CrossRef]

13.  Narayanan, M.; Kiran, A.; Natarajan, D.; Kandasamy, S.; Shanmugam, S.; Alshiekheid, M.; Almoallim, H.S.; Pugazhendhi, A. The pharmaceutical potential of crude ethanol leaf extract of *Pedalium murex* (L.). *Process Biochem.* **2022**, *112*, 234–240. [CrossRef]

14.  Khan, A.; Alamry, K.A. Recent advances of emerging green chitosan-based biomaterials with potential biomedical applications: A review. *Carbohydr. Res.* **2021**, *506*, 108368. [CrossRef] [PubMed]

15.  Li, J.; Cai, C.; Li, J.; Li, J.; Li, J.; Sun, T.; Wang, L.; Wu, H.; Yu, G. Chitosan-based nanomaterials for drug delivery. *Molecules* **2018**, *23*, 2661. [CrossRef]

16.  Prema, P.; Ranjani, S.S.; Kumar, K.R.; Veeramanikandan, V.; Mathiyazhagan, N.; Nguyen, V.-H.; Balaji, P. Microbial synthesis of silver nanoparticles using Lactobacillus plantarum for antioxidant, antibacterial activities. *Inorg. Chem. Commun.* **2022**, *136*, 109139. [CrossRef]

17.  Mehnath, S.; Das, A.K.; Verma, S.K.; Jeyaraj, M. Biosynthesized/Green-Synthesized Nanomaterials as Potential Vehicles for Delivery of Antibiotics/Drugs. In *Comprehensive Analytical Chemistry*; Elsevier: Amsterdam, The Netherlands, 2021; Volume 94, pp. 363–432.

18.  Yang, Y.; Lu, Y.T.; Zeng, K.; Heinze, T.; Groth, T.; Zhang, K. Recent progress on cellulose-based ionic compounds for biomaterials. *Adv. Mater.* **2021**, *33*, 2000717. [CrossRef]

19.  Kakooza-Mwesige, A. The importance of botanical treatments in traditional societies and challenges in developing countries. *Epilepsy Behav.* **2015**, *52*, 297–307. [CrossRef]

20.  Zhang, Y.; Yang, Y.; Shang, Y.; Liang, C.; He, J.; Li, J.; Chang, Y. Optimization of the Purifying Process for Columbianetin-β-D-Glucopyranoside from Angelicae Pubescentis Radix and Evaluation of Its Analgesic Activity Using Hot Plate Test. *Evid.-Based Complement. Altern. Med.* **2021**, *2021*, 9944270. [CrossRef]

21.  Anand, M.; Sathyapriya, P.; Maruthupandy, M.; Beevi, A.H. Synthesis of chitosan nanoparticles by TPP and their potential mosquito larvicidal application. *Front. Lab. Med.* **2018**, *2*, 72–78. [CrossRef]

22.  Roy, S.; Rao, K.; Bhuvaneswari, C.; Giri, A.; Mangamoori, L.N. Phytochemical analysis of Andrographis paniculata extract and its antimicrobial activity. *World J. Microbiol. Biotechnol.* **2010**, *26*, 85–91. [CrossRef]

23.  Soni, A.; Sosa, S. Phytochemical analysis and free radical scavenging potential of herbal and medicinal plant extracts. *J. Pharmacogn. Phytochem.* **2013**, *2*, 22–29.

24.  Narayanan, M.; Divya, S.; Natarajan, D.; Senthil-Nathan, S.; Kandasamy, S.; Chinnathambi, A.; Alahmadi, T.A.; Pugazhendhi, A. Green synthesis of silver nanoparticles from aqueous extract of *Ctenolepis garcini* L. and assess their possible biological applications. *Process Biochem.* **2021**, *107*, 91–99. [CrossRef]

25.  Shao, T.; Yuan, P.; Zhu, L.; Xu, H.; Li, X.; He, S.; Li, P.; Wang, G.; Chen, K. Carbon nanoparticles inhibit α-glucosidase activity and induce a hypoglycemic effect in diabetic mice. *Molecules* **2019**, *24*, 3257. [CrossRef] [PubMed]

26.  Hopf, N.; Champmartin, C.; Schenk, L.; Berthet, A.; Chedik, L.; Du Plessis, J.; Franken, A.; Frasch, F.; Gaskin, S.; Johanson, G. Reflections on the OECD guidelines for in vitro skin absorption studies. *Regul. Toxicol. Pharmacol.* **2020**, *117*, 104752. [CrossRef]

27.  Kaushik, S.; Jain, P.; Satapathy, T.; Purabiya, P.; Roy, A. Evaluation of anti-arthritic and anti-inflammatory activities of *Martynia annua* L. Ethanolic extract. *Clin. Phytosci.* **2021**, *7*, 7.

28.  Macchioni, V.; Carbone, K.; Cataldo, A.; Fraschini, R.; Bellucci, S. Lactic acid-based deep natural eutectic solvents for the extraction of bioactive metabolites of *Humulus lupulus* L.: Supramolecular organization, phytochemical profiling and biological activity. *Sep. Purif. Technol.* **2021**, *264*, 118039. [CrossRef]

29.  Vaezifar, S.; Razavi, S.; Golozar, M.A.; Karbasi, S.; Morshed, M.; Kamali, M. Effects of some parameters on particle size distribution of chitosan nanoparticles prepared by ionic gelation method. *J. Clust. Sci.* **2013**, *24*, 891–903. [CrossRef]

30.  Oh, J.-W.; Chun, S.C.; Chandrasekaran, M. Preparation and in vitro characterization of chitosan nanoparticles and their broad-spectrum antifungal action compared to antibacterial activities against phytopathogens of tomato. *Agronomy* **2019**, *9*, 21.

31.  Rai, S.; Dutta, P.; Mehrotra, G. Lignin incorporated antimicrobial chitosan film for food packaging application. *J. Polym. Mater.* **2017**, *34*, 171.

32.  Singh, J.; Soni, R. Controlled synthesis of CuO decorated defect enriched ZnO nanoflakes for improved sunlight-induced photocatalytic degradation of organic pollutants. *Appl. Surf. Sci.* **2020**, *521*, 146420.

33.  Abdallah, Y.; Liu, M.; Ogunyemi, S.O.; Ahmed, T.; Fouad, H.; Abdelazez, A.; Yan, C.; Yang, Y.; Chen, J.; Li, B. Bioinspired green synthesis of chitosan and zinc oxide nanoparticles with strong antibacterial activity against rice pathogen *Xanthomonas oryzae* pv. *oryzae*. *Molecules* **2020**, *25*, 4795. [CrossRef] [PubMed]

34.  Singh, J.; Dutta, T.; Kim, K.-H.; Rawat, M.; Samddar, P.; Kumar, P. 'Green'synthesis of metals and their oxide nanoparticles: Applications for environmental remediation. *J. Nanobiotechnol.* **2018**, *16*, 84.

35. Cao, C.; Kim, E.; Liu, Y.; Kang, M.; Li, J.; Yin, J.-J.; Liu, H.; Qu, X.; Liu, C.; Bentley, W.E. Radical scavenging activities of biomimetic catechol-chitosan films. *Biomacromolecules* **2018**, *19*, 3502–3514. [CrossRef]

36. Shen, W.; Yan, M.; Wu, S.; Ge, X.; Liu, S.; Du, Y.; Zheng, Y.; Wu, L.; Zhang, Y.; Mao, Y. Chitosan nanoparticles embedded with curcumin and its application in pork antioxidant edible coating. *Int. J. Biol. Macromol.* **2022**, *204*, 410–418. [CrossRef] [PubMed]

37. Kumar, S.P.; Birundha, K.; Kaveri, K.; Devi, K.R. Antioxidant studies of chitosan nanoparticles containing naringenin and their cytotoxicity effects in lung cancer cells. *Int. J. Biol. Macromol.* **2015**, *78*, 87–95.

38. Islam, M.S.; Rashid, M.M.; Ahmed, A.A.; Reza, A.A.; Rahman, M.A.; Choudhury, T.R. The food ingredients of different extracts of *Lasia spinosa* (L.) Thwaites can turn it into a potential medicinal food. *NFS J.* **2021**, *25*, 56–69. [CrossRef]

39. Pal, A.; Goswami, R.; Roy, D.N. A critical assessment on biochemical and molecular mechanisms of toxicity developed by emerging nanomaterials on important microbes. *Environ. Nanotechnol. Monit. Manag.* **2021**, *16*, 100485.

40. Huang, M.; Khor, E.; Lim, L.-Y. Uptake and cytotoxicity of chitosan molecules and nanoparticles: Effects of molecular weight and degree of deacetylation. *Pharm. Res.* **2004**, *21*, 344–353.

41. Loutfy, S.A.; El-Din, H.M.A.; Elberry, M.H.; Allam, N.G.; Hasanin, M.; Abdellah, A.M. Synthesis, characterization and cytotoxic evaluation of chitosan nanoparticles: In vitro liver cancer model. *Adv. Nat. Sci. Nanosci. Nanotechnol.* **2016**, *7*, 035008. [CrossRef]

42. Elkeiy, M.M.; Khamis, A.A.; El-Gamal, M.M.; Abo Gazia, M.M.; Zalat, Z.A.; El-Magd, M.A. Chitosan nanoparticles from Artemia salina inhibit progression of hepatocellular carcinoma in vitro and in vivo. *Environ. Sci. Pollut. Res.* **2020**, *27*, 19016–19028.

43. Philippe, L.; Tosca, L.; Zhang, W.L.; Piquemal, M.; Ciapa, B. Different routes lead to apoptosis in unfertilized sea urchin eggs. *Apoptosis* **2014**, *19*, 436–450. [CrossRef] [PubMed]

44. Mwakalukwa, R.; Amen, Y.; Nagata, M.; Shimizu, K. Postprandial hyperglycemia lowering effect of the isolated compounds from olive mill wastes—An inhibitory activity and kinetics studies on α-glucosidase and α-amylase enzymes. *ACS Omega* **2020**, *5*, 20070–20079. [CrossRef] [PubMed]

45. Sudhakar, K.; Mishra, V.; Hemani, V.; Verma, A.; Jain, A.; Jain, S.; Charyulu, R.N. Reverse pharmacology of phytoconstituents of food and plant in the management of diabetes: Current status and perspectives. *Trends Food Sci. Technol.* **2021**, *110*, 594–610. [CrossRef]

46. Hao, W.; Wang, M.; Lv, M. The inhibitory effects of Yixing black tea extracts on A-glucosidase. *J. Food Biochem.* **2017**, *41*, e12269. [CrossRef]

47. Wang, C.; Chen, P.-X.; Xiao, Q.; Yang, Q.-M.; Weng, H.-F.; Zhang, Y.-H.; Xiao, A.-F. Chitosan activated with genipin: A nontoxic natural carrier for tannase immobilization and its application in enhancing biological activities of tea extract. *Mar. Drugs* **2021**, *19*, 166. [CrossRef]

48. Kuempel, E.D.; Jaurand, M.-C.; Møller, P.; Morimoto, Y.; Kobayashi, N.; Pinkerton, K.E.; Sargent, L.M.; Vermeulen, R.C.; Fubini, B.; Kane, A.B. Evaluating the mechanistic evidence and key data gaps in assessing the potential carcinogenicity of carbon nanotubes and nanofibers in humans. *Crit. Rev. Toxicol.* **2017**, *47*, 1–58. [CrossRef]

49. De Lima, R.; Feitosa, L.; Pereira, A.D.E.S.; De Moura, M.R.; Aouada, F.A.; Mattoso, L.H.C.; Fraceto, L.F. Evaluation of the genotoxicity of chitosan nanoparticles for use in food packaging films. *J. Food Sci.* **2010**, *75*, N89–N96. [CrossRef]

50. Bajpai, V.K.; Kamle, M.; Shukla, S.; Mahato, D.K.; Chandra, P.; Hwang, S.K.; Kumar, P.; Huh, Y.S.; Han, Y.-K. Prospects of using nanotechnology for food preservation, safety, and security. *J. Food Drug Anal.* **2018**, *26*, 1201–1214. [CrossRef]